

Reversed Hofmeister series - the rule rather than the exception

Nadine Schwierz, Dominik Horinek, Uri Sivan, Roland R. Netz

Angaben zur Veröffentlichung / Publication details:

Schwierz, Nadine, Dominik Horinek, Uri Sivan, and Roland R. Netz. 2016. "Reversed Hofmeister series - the rule rather than the exception." *Current Opinion in Colloid & Interface Science* 23: 10–18. <https://doi.org/10.1016/j.cocis.2016.04.003>.

Reversed Hofmeister Series - the Rule rather than the Exception

Nadine Schwierz

Chemistry Department, University of California, Berkeley, California 94720, United States

Dominik Horinek

Institut für Physikalische und Theoretische Chemie, Universität Regensburg, 93040 Regensburg, Germany

Uri Sivan

Department of Physics and the Russell Berrie Nanotechnology Institute, Technion-Israel Institute of Technology, Haifa 32000, Israel

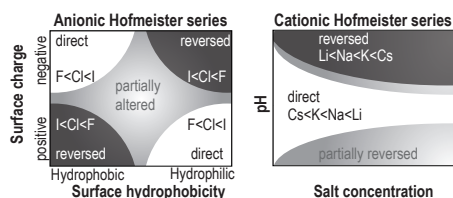
Roland R. Netz

Fachbereich für Physik, Freie Universität Berlin, 14195 Berlin, Germany

Abstract

Over recent years, the supposedly universal Hofmeister series has been replaced by a diverse spectrum of direct, partially altered and reversed series. This review aims to provide a detailed understanding of the full spectrum by combining results from molecular dynamics simulations, Poisson-Boltzmann theory and AFM experiments. Primary insight into the origin of the Hofmeister series and its reversal is gained from simulation-derived ion-surface interaction potentials at surfaces containing non-polar, polar and charged functional groups for halide anions and alkali cations. In a second step, the detailed microscopic interactions of ion, water and functional surface groups are incorporated into Poisson-Boltzmann theory. This allows us to quantify ion-specific binding affinities to surface groups of varying polarity and charge, and to provide a connection to the experimentally measured long-ranged electrostatic forces that stabilize colloids, proteins and other particles against precipitation. Based on the stabilizing efficiency, the direct Hofmeister series is obtained for negatively charged hydrophobic surfaces. Hofmeister series reversal is induced by changing the sign of the surface charge from negative to positive, by changing the nature of the functional surface groups from hydrophobic to hydrophilic, by increasing the salt concentration, or by changing the pH. The resulting diverse spectrum reflects that alterations of Hofmeister series are the rule rather than the exception and originate from the variation of ion-surface interactions upon changing surface properties.

Keywords: Hofmeister series, reversal, surface charge, salt concentration, hydrophobicity, pH, Poisson-Boltzmann theory, molecular dynamics simulations, AFM



Email address: nadine.schwierz@ph.tum.de (Nadine Schwierz)

1. Introduction

Most processes in electrolyte solutions depend not only on the salt concentration or valency of the ions but also on ion type. These ion specific effects are ubiquitous and appear in a large variety of physical properties such as osmotic coefficients, solubility of gases and colloids, protein precipitation and crystallization, catalysis of chemical reactions or enzyme activity [1], suggesting a common origin of these vastly different phenomena [2–9]. In most cases, anions and cations can be ranked reproducibly in a Hofmeister series according to their influence on these macroscopic properties [10]. Due to the widespread applicability and robustness of the same series in bulk, as characterized for example by the ionic solvation free energy, ion specific effects have traditionally been attributed to changes that ions provoke in the surrounding water. However, this simple explanation and the universality of the Hofmeister series have been called into question based on two important observations: First, recent experiments have demonstrated that ions do not perturb the water hydrogen bonding network beyond their first hydration shell [11–13]. Therefore, it is unlikely that the series originates solely from structuring effects of water induced by ions. Consequently, direct ion-macromolecule interactions are more important for ion specific phenomena than bulk ion properties [14–16]. Secondly, over the past years a diverse spectrum of direct, altered and reversed Hofmeister series has been discovered that is not mirrored by a similar modification of the bulk series. Dependent on parameters like surface charge, surface polarity, temperature, salt concentration, pH, and buffer type the ordering of the ions within the series can be changed [17–23]. To give a few explicit examples, the aggregation of negatively charged proteins and colloids follows the usual direct Hofmeister series while cationic proteins [19, 24–26] and cationic colloids [27, 28] show the opposite ordering. In colloidal systems, which allow to independently control surface polarity and surface charge, yet another reversal occurs when changing the surface properties of the particles from hydrophobic to hydrophilic [27–29]. Finally, Hofmeister series reversal by pH has also been observed for surfaces containing dissociable functional groups [23, 30–33].

This lack of universality of the Hofmeister series has changed our current understanding of the series origin. By now, we know that ion specific effects are caused by ion accumulation or depletion from the solute/water interface [34]. Therefore, it is not surprising that the ion-surface affinity, and therefore the ranking in the Hofmeister series, changes if surface properties like hydrophobicity, charge, or chemical structure of surface groups are varied [35, 36]. However, the detailed mechanism by which ions are attracted to or repelled from interfaces is complex and results from the competition of direct ion-surface and indirect hydration-related interactions [37]. For simple non-polar surfaces like the air/water interface or the interface between water and a hydrophobic solid or liquid, the adsorption propensity of large anions such as iodide [38, 39] can be rationalized in terms of hydrophobic solvation theory adapted to interfaces [40–43]. Some theories discuss the enhanced surface affinity also in terms of the ion polarizability [42, 44], which is proportional to the ion volume and thus scales similarly as the hydrophobic solvation contribution. Ion accumulation and depletion at interfaces can be captured by simplified ion-surface interactions, which allow us a global analysis of interfacial ionic distributions and ion specific behavior [45]. However, a general theory that quantifies ion-surface interactions and encompasses hydrophobic as well as hydrophilic surfaces is still missing, due to the complex interactions between surface groups, ions and water. An indispensable tool for gaining insight into the adsorption propensity of ions to different interfaces are all-atom molecular dynamics (MD) simulations in explicit water, which account for the subtle interplay of ion hydration in bulk and partial ion dehydration upon surface binding. Effective ion-surface interactions can be derived from these simulations [38, 44, 46, 47] and incorporated into multiscale theories [44, 46, 48], thereby providing a link between the microscopic adsorption behavior of the ions and macroscopic, experimentally accessible quantities.

In this review, we summarize our recent work and provide insight into the full spectrum of direct, reversed, and altered anionic and cationic Hofmeister series. In particular, we uncover the effects of surface charge, surface hydrophobicity and pH on the ordering of halide anions and alkali cations. First, detailed insight into the interplay of direct ion-surface interactions and the role of ion hydration is derived from all-atom MD simulations in explicit water at surfaces containing non-polar methyl (CH_3), polar hydroxide (OH), polar carboxyl (COOH), and charged carboxylate (COO^-) surface groups. Ion specific binding affinities to the different surface groups are quantified by calculation of the free energy profile or potential of mean force (PMF) underlying ion adsorption or depletion. For anions, a clear reversal of the surface affinity is observed

if non-polar surface groups are replaced by polar or charged groups. For cations, a diverse spectrum of direct, reversed and partially reversed series based on single-ion binding affinities to non-polar, polar and charged groups is encountered, which makes cations less regular compared to anions. In a second step, the ion-surface interaction potentials are embedded into Poisson-Boltzmann theory to yield the ranking of anions and cations based on macroscopic quantities. In particular, the long-ranged electrostatic forces, which stabilize solutes against precipitation due to van-der-Waals attraction, are quantified in different electrolyte solutions and compared to precise AFM measurements of forces between silica surfaces. Based on these forces, the direct Hofmeister series is obtained for negatively charged non-polar surfaces. Hofmeister series reversal or partial alterations are induced by changing the sign of the surface charge from negative to positive, by changing the nature of the functional surface groups from hydrophobic to hydrophilic, by increasing salt concentration, or by changing the pH for surfaces containing acidic surface groups. In all cases, Hofmeister series reversal emerges as a direct consequence of specific ion adsorption at the surface leading to enhancement or reduction of the effective surface charge and the associated electrostatic force of stabilization.

2. Methods

2.1. Simulations and Poisson-Boltzmann theory

Multiscale modeling approach: We use a two-step modeling approach that has been described in detail in Ref. [33, 43, 46]. Briefly, in the first step, explicit solvent molecular dynamics (MD) simulations are used to calculate single ion-surface interaction potentials for halide anions and alkali cations at surfaces containing hydrophobic methyl (CH_3), polar hydroxide (OH), polar carboxyl (COOH), and charged carboxylate (COO^-) surface groups. In the second step, these interaction potentials are imported into Poisson-Boltzmann theory to calculate the ionic density profiles and the electrostatic potential at surfaces of arbitrary charge and for finite ion concentrations.

MD simulations: In the simulations the surface is a $3.5 \times 3.46 \text{ nm}^2$ self-assembled monolayer (SAM) consisting of 56 $\text{C}_{20}\text{H}_{41}$ chains with different terminal groups. The simulation box has an extension of 9 nm in the z -direction and is filled with about 2,700 SPC/E water molecules. The SAM is modeled with the GROMOS96 force field [49]. To ensure correct ion-water and ion-ion interactions, we use previously optimized force field parameters for anions and cations [50] that reproduce thermodynamic solvation properties and yield accurate ion pairing properties as judged by comparison with experimental osmotic coefficient data [51]. The simulations are done at a temperature of 300 K and a pressure of $P_z=1$ bar maintained by anisotropic pressure coupling, corresponding to the NAP_zT ensemble using the Gromacs simulation package [52]. Periodic boundary conditions are applied, long range Coulomb forces are calculated using the particle-mesh Ewald summation [53] and for the van-der-Waals interactions a cutoff radius of 1.2 nm is used. A single ion is placed into the water phase and its potential of mean force (PMF) is calculated by umbrella sampling [54] with a window spacing of 0.025 nm and 3-10 ns simulation time discarding the first 1 ns for equilibration. A time step of 2 fs and the weighted histogram analysis method [55] with force constant $k_z = 1000 \text{ kJ}/(\text{mol nm}^2)$ is used. For the charged surface, we use an additional two-dimensional harmonic potential with $k_{\text{B}}T/k_{x,y} = 0.0145 \text{ nm}^2$ to laterally confine the ion above the charged group.

Poisson-Boltzmann modeling: In our multiscale modeling we consider two limiting scenarios for the surface charge density. In the first scenario, we assume evenly distributed charges and the chemical structure of the surface groups remains unchanged. In this scenario, we allow both polar hydroxide and non-polar methyl surface groups to carry a net charge. This corresponds to a situation where the charge is distributed evenly over the surface and can be realized experimentally by using back-gated semiconductors or self-assembled monolayers [56]. This distinction between surface polarity and surface charge corresponds to an idealized limit and allows us a successful classification in line with a broad range of different colloidal surfaces [27, 28]. In the second scenario, we model the pH dependent deprotonation of carboxylic surface groups. Thereby, we not only change the surface charge density but also the chemical structure of the surface group. Here, the surface acquires charges by deprotonation. Prominent examples are minerals with hydroxide surface groups and proteins with carboxyl surface groups [57]. To account for surfaces of varying

hydrophobicity (scenario 1) or of varying degree of deprotonation (scenario 2), we use a molecular-scale approach, where the effective ion-surface interaction results from the weighted average of the potentials of the polar OH (V_i^{phil}) or non-polar CH₃-groups V_i^{phob} and the uncharged COOH (V_i^{COOH}) or charged COO⁻-groups ($V_i^{\text{COO}^-}$) [43]. The PB equation including the ion specific PMFs of anions and cations for two different surface groups then reads

$$\epsilon\epsilon_0 \frac{d^2}{dz^2} \Phi(z) = \sum_{i=\pm} q_i c_i(z) \quad (1)$$

For surfaces with varying surface hydrophobicity (scenario 1) the ionic densities are determined by

$$c_{\pm}(z) = c_0 e^{-((1-\alpha)V_{\pm}^{\text{phil}}(z) + \alpha V_{\pm}^{\text{phob}}(z) + q_{\pm}\Phi(z))/k_B T} \quad (2)$$

and for surfaces containing dissociable carboxyl groups (scenario 2) the densities are determined by

$$c_{\pm}(z) = c_0 e^{-((1-\xi)V_{\pm}^{\text{COOH}}(z) + \xi V_{\pm}^{\text{COO}^-}(z) + q_{\pm}\Phi(z))/k_B T}. \quad (3)$$

Here, z is the distance perpendicular to the surface, q_i is the charge of ions of type i , c_0 is the bulk salt concentration, ϵ_0 is the dielectric constant of vacuum, ϵ is the relative dielectric constant of water, and $\Phi(z)$ is the electrostatic potential. The parameter α in Eq 2 is the surface hydrophobicity and corresponds to the fraction of hydrophobic CH₃-surface groups. The parameter ξ in Eq 3 is the degree of deprotonation and corresponds to the fraction of charged COO⁻-groups on the surface. Eq 1 is solved numerically on a one-dimensional grid with a lattice constant of 1 pm yielding the ion concentration profiles $c_{\pm}(z)$ perpendicular to the surface and the electrostatic potential $\Phi(z)$ in dependence of the parameters ξ and α and bulk salt concentration c_0 . The potential satisfies the bulk boundary condition $\Phi(z \rightarrow \infty) = 0$. In addition, we use the constant charge boundary condition $d\Phi(z)/dz = -\sigma_{\text{surf}}/\epsilon_0\epsilon$ at the surface located at $z = 0$. The surface position $z = 0$ is defined by the mean position of the surface oxygen atoms for polar surfaces and thus reflects the fact that the surface charge is localized in the oxygen atoms. For the non-polar surfaces, we define $z = 0$ as the mean position of the terminal carbon atoms. For scenario 2 defined by Eq 3, the surface boundary condition can be rewritten in terms of the deprotonation degree ξ as $d\Phi(z)/dz|_{z=0} = -\xi\sigma_{\text{COO}}/\epsilon_0\epsilon$, where $\sigma_{\text{COO}} = -4.624 \text{ e/nm}^2$ corresponds to the surface charge density of the COO⁻-group.

Modified Fermionic Poisson-Boltzmann modeling: To ensure that the ionic density does not exceed its physical limit, set by the ionic volume, the hard-core repulsion between ions must be included. In the simplest approach, the proper ionic densities $c_{\pm}(z)$ are calculated from the unrestricted ionic densities for anions $\tilde{c}_-(z)$ and cations $\tilde{c}_+(z)$ using the Fermionic distribution[58, 59]

$$c_{\pm}(z) = \frac{\sqrt{2}\tilde{c}_{\pm}(z)}{\sqrt{2} + a_{\pm}^3(\tilde{c}_{\pm}(z) - c_0) + a_{\mp}^3(\tilde{c}_{\mp}(z) - c_0)} \quad (4)$$

with the effective diameters of positive and negative ions a_+ and a_- taken from the first peak in the ion-water radial distribution function obtained in previous simulations [43]. Eq 4 restricts the maximum density to $a_{\pm}^{-3}\sqrt{2}$ corresponding to the maximum density of close-packed spheres with diameter a_{\pm} . Steric effects become important at large salt concentrations, high surface charge densities and for large ion-surface interaction strengths. As before, the unrestricted ionic densities $\tilde{c}_{\pm}(z)$ follow from the Boltzmann distribution

$$\tilde{c}_{\pm}(z) = c_0 e^{-((1-\xi)V_{\pm}^{\text{COOH}}(z) + \xi V_{\pm}^{\text{COO}^-}(z) + q_{\pm}\Phi(z))/k_B T}. \quad (5)$$

Combining eq 1, 4 and 5 yields the modified Poisson-Boltzmann equation that will be used for the carboxylic surfaces.

The pH as function of the degree of dissociation is determined according to the self-consistent equation

$$\text{pH} = \log \frac{\xi}{1-\xi} + \text{pK}_a - \frac{e\Phi(z_H)}{2.303k_B T}. \quad (6)$$

The last term is the electrostatic contribution that takes ion specificity into account via the ion type dependent surface potential at the position of the surface protons z_H , without this term the ordinary equation for the acid deprotonation equilibrium in bulk solution is obtained. In the following we assume a pK_a value of 4.76 for monolayers with COOH -groups [60].

2.2. Experimental setup

A 5 μm diameter silica colloid (Bangs Labs) was glued onto a gold-coated, silicon nitride AFM cantilever (Bruker MLCT-O10). The cantilever, along with a pristine silicon substrate (Siltronix -100) underwent 30-second plasma oxidation (PlasmaTherm 790 RIE) at 50 Watts RF power, and 50 mTorr O_2 gas. Measurements of the force between the colloid and the substrate in the presence of several solutions were performed under moderate, steady flow through a fluid cell (Bruker MTFML) using a commercial AFM (Bruker - Multimode), modified to yield low noise data. Force was determined by multiplying the cantilevers' deflection by their individual spring constant ($\sim 0.05 \text{ N/m}$) as measured by thermal fluctuations. Colloid substrate separation was deduced by calibrating the change in cantilever deflection versus the rise in the piezoelectric stage with the two in contact. All solutions were prepared with analytical grade salts, dissolved in 18 $\text{M}\Omega\text{-cm}$ DI water. The pH was set without buffer, using HCl or M-OH , where M was identical to the electrolyte cation. Dissolved CO_2 was expelled from the solution by bubbling high purity Nitrogen gas immediately preceding the measurements. The solution pH was monitored in real time with a glass pH electrode sampling the solution in-situ in a sealed holder, immediately down-stream from the fluid cell. We note that pH electrodes are known to be ion specific. However, at our salt concentrations, this effect is expected to be smaller than 0.1 pH unit [61], namely, smaller than our perceived error. Measurements in pure saline solutions titrated with hydrochloric acid to pH 5.5 were identical to those measured at the same pH in the presence of atmospheric CO_2 buffering. The sample surfaces were soaked in 1M NaCl solution for 30 minutes prior to the experiment. We have found that this procedure generally increases surface charge and improves sample stability and reproducibility. Force curves were acquired with slow approach velocities ($\sim 100 \text{ nm/s}$) to avoid hydrodynamic effects. At the end of every set of measurements, a reference force vs. distance curve was measured in 1mM NaCl solution at pH 5.5 and verified to coincide with an identical measurement taken at the beginning of the set.

3. Results and Discussion

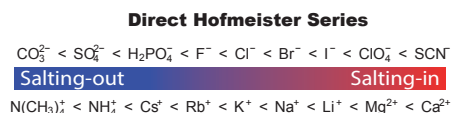


Figure 1: Standard direct Hofmeister series for anions and cations based on precipitation studies of negatively charged proteins [16, 34]. To the left, ions have the smallest stabilization power and salt-out proteins. To the right, ions have the highest stabilization power and salt-in proteins.

Figure 1 shows the generally accepted *direct Hofmeister series* for anions and cations [14, 16, 34], which orders the ions with respect to macroscopic properties like surface tension, solubility of hydrocarbons, protein denaturation, or protein stability. To the left, the stabilization power against precipitation is smallest and one obtains salting-out behavior. To the right, the stabilization power is highest and salting-in behavior is displayed. At the same time, ions to the left tend to be structure-stabilizers, conserving the native structure of proteins, while ions to the right tend to be denaturants. The different binding affinities of ions to hydrophobic surface patches govern both ion specific protein precipitation [35] and denaturation [37, 62] and explain both processes via essentially the same mechanism: Ions that are strongly repelled from hydrophobic surfaces (such as F^-) raise the interfacial tension strongly. Therefore, proteins in solution minimize their solvent exposed surface area by folding into compact structures (native structure stabilizers) and by aggregation (strong precipitators). On the contrary, ions that adsorb to hydrophobic surfaces (such

as I^-) decrease the interfacial tension. Therefore, proteins maximize the solvent exposed surface area by unfolding (denaturants) and segregation (stabilizers). It transpires that the direct Hofmeister series in Figure 1 holds for hydrophobic surfaces that are charge neutral or have a bare negative charge. As turns out, most biological and technologically relevant surfaces are of this type, which explains the prevalence of this ion ordering. Since ion binding or depletion at interfaces is essential for a detailed understanding of Hofmeister effects, we will discuss single-ion binding to hydrophobic, hydrophilic and charged surface groups in the following.

3.1. Ion-surface binding affinities - reversal of the Hofmeister series at the single-ion level for hydrophobic and hydrophilic surfaces

Detailed insight into the distributions of anions and cations can be obtained from MD simulations for instance at the air/water interface [38, 39, 41, 44, 47], at atomistically resolved peptide and protein surfaces [63, 64] or at the solid/water interface of surfaces containing different functional groups [33, 43, 46]. The surface affinities of halide anions and alkali cations at surfaces containing hydrophobic methyl (CH_3), polar hydroxide (OH), polar carboxyl (COOH), and charged carboxylate (COO^-) terminal groups are summarized in Table 1 [33, 43, 46]. For anions, a clear reversal of the single-ion binding affinity takes place when comparing hydrophobic and hydrophilic surfaces. For cations, the situation is more complex and a broad spectrum of direct, reversed and partially altered series is observed. To gain a detailed understanding of the microscopic surface affinity, we discuss ion-surface interactions for the example of hydrophobic CH_3 -terminated and polar OH -terminated surfaces in more detail.

The single-ion surface affinity is quantified by calculating the free energy profile (the so called potential of mean force PMF) underlying ion adsorption at the two different surfaces (Figure 2A, B). At the hydrophobic surface, the surface affinity of the ions correlates with their size. The largest cation Cs^+ and the largest anion I^- adsorb strongest and the surface affinity decreases with decreasing ion size: $\text{Cs}^+ > \text{K}^+ > \text{Na}^+$ and $\text{I}^- > \text{Cl}^- > \text{F}^-$. The higher surface affinity of large ions can be rationalized by hydrophobic solvation theory, in which the surface affinity scales with the size of the ion [40–43]. The behavior of Li^+ is more complex since its first hydration shell stays intact for all separations from the surface [43]. At the hydrophobic surface, Li^+ behaves like an ion with effectively larger radius and the alterations in the PMF result from a compression of the second hydration shell [43]. At the same time, large anions and cations shed off the hydration water molecules facing the hydrophobic surface (Figure 2C for Cs^+ and I^-) and preferentially adsorb (minimum in the free energy profile in Figure 2A, B) while the smaller ions preferentially retain their hydration shell and tend to be repelled from the hydrophobic interface.

The situation changes if the hydrophobic surface is replaced by the hydrophilic OH -terminated surface: the anion affinity is reversed and specificity is less pronounced [46]. Here, the small F^- ion is least repelled and the surface affinity decreases with increasing ion size: $\text{F}^- > \text{Cl}^- > \text{I}^-$. The reversed surface affinity can be rationalized with the law of matching water affinities [65]: Anions preferentially interact with the small hydrogen on the OH -group, which has a high surface charge density. Therefore, small ions like F^- adsorb preferentially and can simultaneously form contact pairs with several surface hydrogen atoms. These rather stable configurations counterbalance the loss of strongly bound hydration water and the cost for partial ion dehydration. The situation is more complex for cations (Figure 2A): At the OH -terminated surface, small cations preferentially interact with the oxygen atoms, which have an intermediate surface charge density and the surface affinity is highest for Li^+ and lowest for K^+ , while Cs^+ interacts favorably at large surface separations, corresponding to a partially reversed series.

In summary, ion adsorption or repulsion from an interface results from direct ion-surface interactions and the subtle interplay of ion hydration in bulk and the cost of partial ion dehydration upon surface binding. However, up to now no theory exists that accurately accounts for all interactions involved and robustly predicts the ion specific binding free energy at different surfaces. Therefore, all-atom MD simulations will likely continue to be an indispensable tool to obtain atomistic insight into ion specific phenomena at interfaces.

Table 1: Ion specific affinities for surfaces with different functional groups: hydrophobic methyl (CH_3), polar hydroxide (OH), polar carboxyl (COOH), and charged carboxylate (COO^-) groups. The ranking shows the ordering of anions and cations according to their surface binding affinities based on single-ion free energy profiles and interfacial tensions [33, 43, 46].

Functional group	anion binding affinity	cation binding affinity
CH_3	$\text{I}^- > \text{Cl}^- > \text{F}^-$	$\text{Cs}^+ > \text{Li}^+ > \text{K}^+ > \text{Na}^+$
OH	$\text{F}^- > \text{Cl}^- > \text{I}^-$	$\text{Li}^+ > \text{Cs}^+ > \text{Na}^+ > \text{K}^+$
COOH	$\text{F}^- > \text{Cl}^- > \text{I}^-$	$\text{Cs}^+ > \text{Na}^+ > \text{Li}^+$
COO^-	$\text{F}^- \gtrsim \text{Cl}^- \gtrsim \text{I}^-$	$\text{Li}^+ > \text{Na}^+ > \text{Cs}^+$

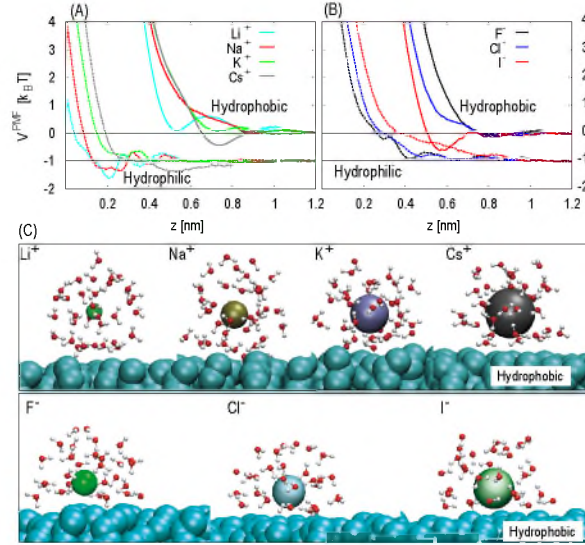


Figure 2: Free energy profiles (PMFs) for cations (A) and anions (B) at the hydrophobic surface (solid lines) and the hydrophilic surface (dotted lines) in dependence of the ion-surface separation z . The PMFs at the hydrophilic surface are shifted vertically for clarity. (C) Simulation snapshots at the hydrophobic surface. Top: Cations at $z = 0.75$ nm (minimum in the PMF of Cs^+). Bottom: Anions at $z = 0.575$ nm (minimum in the PMF of I^-). Water molecules within 6 Å of the ions are shown and ionic sizes correspond to their Pauling radii.

3.2. Stabilizing long-ranged repulsive forces due to specific ion adsorption

The stability of solutes like colloids or proteins in an electrolyte solution results from a balance of electrostatic repulsion and van-der-Waals attraction. In the following, we quantify the stabilizing long-ranged forces in different salt solutions from simulations and experiments and provide a connection between the microscopic adsorption of the ions at surfaces and the macroscopic stabilization efficiency. In the setup considered by us (schematically shown in the inset of Figure 3B), the force between a colloidal particle and an extended surface at separation D is given by [60]

$$\frac{F(D)}{R} = 2\pi \left(-H/(12\pi D^2) + 2\epsilon\epsilon_0\kappa\Phi_{\text{DH}}^2 e^{-\kappa D} \right). \quad (7)$$

In the following, we assume a constant dielectric profile at the interface, since the dielectric constant is only modified in a thin sub-nanometer thick interfacial layer [66] and neglect the decrease of the dielectric constant with increasing salt concentration due to the collective water-water decorrelation effects [67]. The first term in equation 7 corresponds to van-der-Waals attraction characterized by the Hamaker constant $H = 2.2 \times 10^{-21} \text{J}$ for silica surfaces [20]. The second term corresponds to the electrostatic repulsion. The repulsive force results from screened electrostatic interactions of two effectively charged surfaces across an electrolyte solution. The effective charge on the surfaces has two contributions: The bare surface charge and the charge due to specific-ion adsorption which decreases or increases the bare surface charge. The

magnitude of the resulting total effective surface charge σ_{DH} or the equivalent Debye-Hückel potential Φ_{DH} quantify the stabilizing repulsive force. In our Poisson-Boltzmann formalism, Φ_{DH} and σ_{DH} are calculated from the full electrostatic potential $\Phi(z)$ via

$$\Phi_{\text{DH}} = \lim_{z \gg 2 \text{ nm}} (\Phi(z)e^{\kappa z}), \quad \sigma_{\text{DH}} = \epsilon\epsilon_0\kappa\Phi_{\text{DH}}. \quad (8)$$

Note that at very short separations that are of the order of the range of the specific ion adsorption ($D \sim 2$ nm), the microscopic details of the ion-surface interaction potentials become important [45, 46]. Moreover, for unequal pairs of polar/nonpolar surface long-ranged electrostatic attraction occurs [68], which is not further discussed in this review.

Figures 3A, B provide insight into the forces between a silica colloid and a silica surface, obtained from AFM experiments at different salt concentrations. The corresponding forces between two hydrophobic surfaces obtained from the PB modeling are shown in 3C, in which the bare surface charge ($\sigma_{\text{surf}} = -0.022 \text{ e/nm}^2$) was adjusted to match the experimental value [43]. At low salt concentrations (10-50 mM), the force is repulsive and decays exponentially with increasing separation (Figure 3A, C). The effect of van-der-Waals attraction appears only at small separations and is separated by a force maximum from the rather long-ranged repulsive part at low salt concentrations (Figure 3C). However, at high salt concentrations (200 mM), the barrier vanishes and the interaction between the two negatively charged surfaces turns attractive in the presence of Cs^+ (Figure 3B, C). In this concentration regime, the same two objects repel each other in NaCl solution but attract each other in CsCl solution. We conclude that the efficiency of the different salts in stabilizing solutes in electrolyte solutions depends on the magnitude of the repulsive force, which is determined by the magnitude of the stabilizing potential Φ_{DH} or the equivalent effective surface charge σ_{DH} .

The situation is summarized in Figure 3D, which shows σ_{DH}^2 as a function of the bulk salt concentration for a hydrophobic surface with $\sigma_{\text{surf}} = -0.022 \text{ e/nm}^2$. The magnitude of the stabilizing force follows the direct Hofmeister order ($\text{Na}^+ > \text{K}^+ > \text{Li}^+ > \text{Cs}^+$) and is exactly opposite to the surface affinity of the cations since ion adsorption partially neutralizes the negative surface charge (Table 1). The diagram displays a region of attraction, in which the repulsive barrier vanishes, and a region of repulsion, in which van-der-Waals attraction is overcompensated by electrostatic repulsion leading to a repulsive barrier. The crossover from repulsion to attraction at $c_0 = 60 \text{ mM}$ is observed as specific Cs^+ adsorption increasingly neutralizes the bare surface charge and the repulsive force diminishes and gives way to van-der-Waals attraction. With further increasing salt concentration, surface charge reversal takes place (at $c_0 = 200 \text{ mM}$) due to excess adsorbed Cs^+ leading to reemerging repulsion for $c_0 > 950 \text{ mM}$, now between two (effectively) positively charged surfaces. As a matter of fact, the Cs^+ concentration beyond which charge reversal is observed in the experiments is estimated to be slightly less than 200 mM [20].

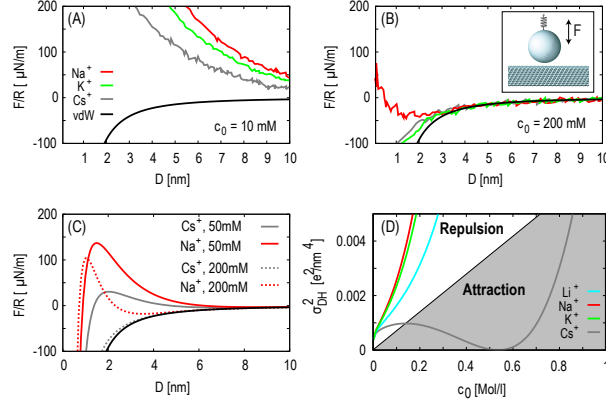


Figure 3: Forces between identical surfaces in different electrolyte solutions. (A) Experimental result for silica: Force between a sphere and a planar surface divided by colloid radius vs separation at pH 5.5 for NaCl, KCl and CsCl at low salt concentrations $c_0 = 10$ mM and at high salt concentrations $c_0 = 200$ mM (B). The inset in (B) shows the schematic setup for the measurements. (C) Simulation results for the force in the plane-sphere setup for hydrophobic surfaces in NaCl and CsCl (with bare surface charge $\sigma_{\text{surf}} = -0.022$ e/nm² adjusted to the experimental results). The force for NaCl exhibits a repulsive range for both concentrations. For CsCl the repulsion observed at low concentration vanishes for $c_0 = 200$ mM. Black lines correspond to pure van der Waals attraction. (D) Theoretical attraction/repulsion diagram for two hydrophobic surfaces with $\sigma_{\text{surf}} = -0.022$ e/nm² based on the effective surface charge σ_{DH} for NaCl (red), KCl (green), CsCl (gray), and LiCl (light blue). The gray area indicates a vanishing repulsive force barrier for CsCl.

3.3. Reversal of the cationic Hofmeister series in dependence of the surface charge and salt concentration

The sign of the surface charge density has a crucial influence on the Hofmeister series. Already in 1911, Hofmeister series reversal has been observed when changing the charge of the precipitating protein [69] and numerous later findings confirmed those observations. In particular, the solubility of negatively charged proteins like hemoglobin follows the direct order for anions and cations [70, 71] while the solubility and crystallization of positively charged proteins like lysozyme follow the reversed order [17, 19, 24]. In fact, the cation ranking in Hofmeister's original work [10] corresponds to what we would now call the indirect series and is representative of cationic proteins.

What is the microscopic reason for reversal of the Hofmeister series dependent on the sign of the surface charge? A pictorial explanation for cations is shown in Figure 4A: At the hydrophobic surface the large Cs⁺ ion adsorbs stronger than Na⁺. At negatively charged surfaces, the bare surface charge is compensated most efficiently by strongly adsorbing cations and the stabilization is therefore smallest for large cations (direct series). In contrast, at a positively charged surface, the surface charge is further enhanced by specific cation adsorption leading to the largest electrostatic stabilization by large cations like Cs⁺ (indirect series). For anions, the picture is opposite: At negatively charged surfaces, the bare surface charge is enhanced further by strongly adsorbing large anions like I⁻ (direct series) while at positively charged surfaces the bare surface charge is compensated most efficiently by adsorption of large anions (indirect series).

The stabilization efficiency of the ions is quantified by calculating the electrostatic force based on Φ_{DH} . Figure 4B shows the full crossover for cations from the direct series (negative σ_{surf}) over two partially reversed series (intermediate σ_{surf}) to the fully reversed series (positive σ_{surf}). For each salt, the stabilizing force decreases with decreasing σ_{surf} until the bare surface charge is exactly canceled by specific ion adsorption (vanishing long-ranged electrostatic repulsion). Beyond this point, Φ_{DH} changes sign (from negative to positive) and repulsion reemerges.

Another crossover from indirect to direct series is observed dependent on the salt concentration (Figure 4C) in agreement with the experimentally observed concentration dependent Hofmeister series reversal for lysozyme [19]. For positively charged solutes, the series is indirect only at low salt concentrations. At higher salt concentration the adsorption of the counter-ion overcompensates the positive charge, leading to effectively negative surfaces in KCl and NaCl solutions (charge reversal is observed at $c_0 = 0.2$ M in Figure 4C). At the same time, the effective charge in CsCl solution is positive but smaller in magnitude leading

again to the direct series at large salt concentrations.

The results are summarized in the cationic Hofmeister phase diagram dependent on the surface charge σ_{surf} and the bulk salt concentration c_0 (Figure 4D). The diagram displays the complete spectrum of direct (white), partially altered (gray) and reversed Hofmeister series (black). The horizontal and vertical dashed lines indicate the full crossover when changing the sign of the surface charge (quantified in Figure 4B) or the bulk salt concentration (quantified in Figure 4C).

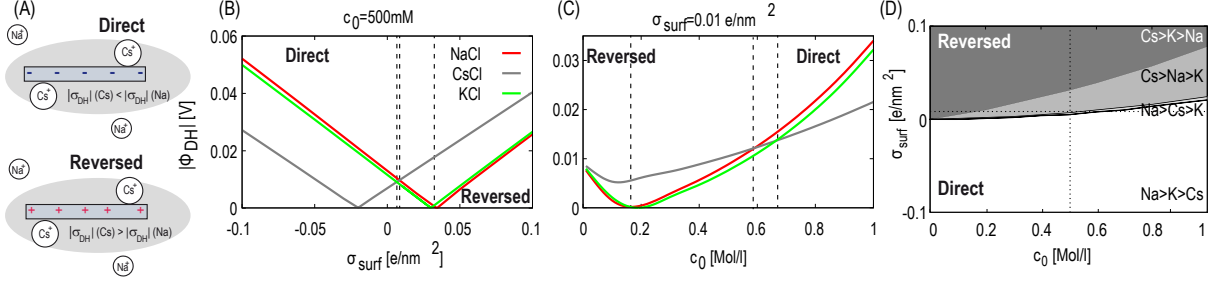


Figure 4: (A) Schematic explanation of the Hofmeister series reversal when changing the sign of the surface charge exemplary for Na^+ and Cs^+ : At the hydrophobic surface Cs^+ adsorbs stronger and is thus drawn closer to the surface. At negatively charged surfaces, the magnitude of the effective surface charge (gray shading) is lower for Cs^+ since specific adsorption partially cancels the negative surface charge: $|\sigma_{\text{DH}}|(\text{Cs}^+) < |\sigma_{\text{DH}}|(\text{Na}^+)$ (direct Hofmeister series according to stabilizing efficiency). At positively charged surfaces, the magnitude of the effective surface charge is further enhanced by Cs^+ adsorption, leading to a stronger long-ranged electrostatic repulsion: $|\sigma_{\text{DH}}|(\text{Cs}^+) > |\sigma_{\text{DH}}|(\text{Na}^+)$ (reversed Hofmeister series). (B) Stabilizing electrostatic force quantified by Φ_{DH} in dependence of the external surface charge σ_{surf} for a constant bulk salt concentration $c_0 = 500$ mM for a hydrophobic surface. A full crossover is observed from the direct series (negative σ_{surf}) to the indirect series (positive σ_{surf}). Dashed lines indicate partial series reversal. (C) Reversal of the Hofmeister series in dependence of the bulk salt concentration for a constant positive surface charge $\sigma_{\text{surf}} = 0.01$ e/nm² for a hydrophobic surface. (D) Hofmeister phase diagram for the cations at the hydrophobic surface in dependence of σ_{surf} and c_0 . Shaded areas denote regions featuring direct series (white), indirect series (black), and two different alteration. The ordering of the ions corresponds to the magnitude of the stabilizing force based on Φ_{DH} . The dotted lines indicate the intersections for which Φ_{DH} is shown in (B) and (C).

3.4. Reversal of the anionic Hofmeister series in dependence of the sign of the surface charge and surface hydrophobicity

Protein surfaces consist of a mixture of polar/non-polar groups or patches. A typical protein surface contains 1/3 hydrophobic and 2/3 hydrophilic groups, while the interior contains only about 1/3 hydrophilic groups mostly associated with the backbone [36]. Similarly, colloids and many other solutes are characterized by varying amounts of mixed hydrophilic and hydrophobic surface groups. Since the contributions of a large variety of different functional groups on ion-specific effects have experimentally been found to be additive [72], the adsorption of ions to surfaces containing a mix of hydrophobic and hydrophilic surface groups can to first approximation be modeled as superposition of ion adsorption at the purely hydrophobic and hydrophilic surface. This opens up the possibility to model complex surfaces consisting of heterogeneous surface groups and to quantify Hofmeister series reversal depending on the fraction of hydrophobic surface groups (equation 2).

The corresponding Hofmeister series phase diagram is shown in Figure 5 for surfaces of varying surface hydrophobicity α and surface charge σ_{surf} for constant bulk salt concentration $c_0 = 200$ mM. The phase diagram shows different regions, in which the anions are ordered based on their stabilizing efficiency. The stabilizing efficiency is quantified by the magnitude of the stabilizing force based on the effective surface potential Φ_{DH} at each point in the $(\sigma_{\text{surf}}, \alpha)$ space [43]. Six different series are observed corresponding to direct order (white), indirect order (black) and four different alterations (gray and blue). The phase diagram is qualitatively symmetric under double reversal of surface charge and surface hydrophobicity and in agreement with the experimentally observed spectrum of Hofmeister series for colloids and proteins [19, 24, 27–29]. The origin of series reversal when changing the surface hydrophobicity is a direct consequence of the reversed surface affinities of the anions when replacing hydrophobic by hydrophilic surface groups (Table 1). The mechanism of series reversal when changing the sign of the surface charge for anions is identical to the mechanism for cations discussed in detail in the previous section and shown schematically in Figure 4A. Series reversal originates from the compensation/enhancement of the bare surface charge σ_{surf} due to specific adsorption of ions with opposite/identical charge. In particular, strongly adsorbing anions like I^- increase the negative surface charge of hydrophobic surfaces further and lead to the highest stabilization. In contrast, at positively charged surfaces strongly adsorbing anions lead to the most efficient charge compensation and therefore to the weakest stabilization.

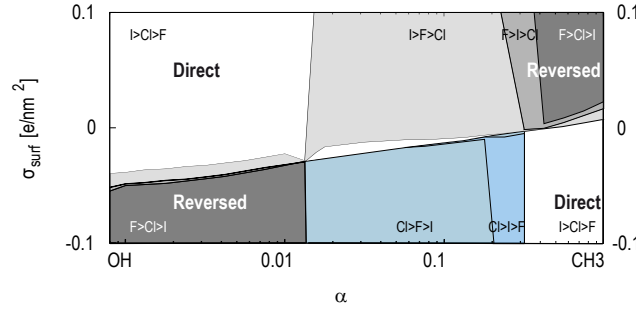


Figure 5: Hofmeister phase diagram for anions and heterogeneous hydrophobic/hydrophilic surfaces in dependence of the bare surface charge σ_{surf} and the surface hydrophobicity α for constant bulk salt concentration $c_0 = 200$ mM. Colored areas denote regions featuring direct order (white), indirect order (black), and four different alterations. The ordering of the anions corresponds to the magnitude of the stabilizing force based on the effective surface potential Φ_{DH} .

3.5. pH dependence of the Hofmeister series

A central mechanism underlying ion specific effects is ion binding to charged surface groups [63]. Depending on pH, acidic groups which are frequently present on the surface of minerals and proteins are either

protonated or deprotonated. Thereby, the surface charge is changed as well as the chemical surface structure, since the presence or absence of surface hydrogens modifies the interaction with surrounding ions and solvation water. Ion specific adsorption is influenced directly by changes in the chemical structure, evident from the reversal of the cation binding affinities to uncharged carboxyl (COOH) surface groups compared to charged carboxylate (COO⁻) surface groups (Table 1 and simulation snapshots in Figure 6A). At low pH, most carboxylic surface groups are protonated and thus charge neutral. For COOH-groups, the partial charges on the surface oxygens are quite low and large cations like Cs⁺ are attracted more strongly than Li⁺ and Na⁺. At high pH most carboxylic groups are deprotonated. For COO⁻-groups, the partial charge on the oxygens is increased, which leads to a stronger attraction of small cations such as Li⁺ and Na⁺ compared to the large Cs⁺ cation.

Stabilization of surfaces containing acidic surface groups results from two processes: deprotonation and ion specific adsorption. The pH dependent Hofmeister series reversal appears as a general fingerprint of acidic surfaces. For example, in Figure 6B, C the effective surface charge σ_{DH} and the corresponding stabilizing force based on the effective surface potential Φ_{DH} is shown for surfaces containing acidic carboxyl groups from our theoretical model (Figure 6B) and for silica surfaces containing acidic silanol groups obtained from our AFM experiments (Figure 6C). Theory and experiments show the same behavior: σ_{DH} decreases monotonically with increasing pH at low pH since more and more acidic groups dissociate and follows the direct Hofmeister series. At a pH of around 8.5 (theory for carboxyl-surface) and 7 (experiments with silica-surface) reversal of the series occurs. This reversal from the direct Hofmeister series at low pH to the reversed series at high pH is a direct consequence of the reversed microscopic binding affinities of the cations to the protonated (low pH) and deprotonated (high pH) form of the acidic surface groups [33].

The efficiency of the different cations in stabilizing surfaces containing acidic surface groups is summarized in the Hofmeister phase diagram dependent on pH and salt concentration (Figure 6D). For intermediate pH values the phase diagram displays an extended region corresponding to the direct Hofmeister series. At high pH values, the observed pH dependent reversal of the Hofmeister series can be understood in terms of the reversed cationic affinities to the protonated and deprotonated carboxylic groups as discussed above: Small Li⁺ ions have a higher affinity than large Cs⁺ ions to the charged carboxylate group, which dominates at high pH. As a consequence, the effective surface charge and the stabilization force at high pH is lower for Li⁺ compared to Cs⁺, corresponding to the reversed Hofmeister series. At intermediate pH values, the situation is opposite. Here, Cs⁺ binds strongest to the neutral carboxyl group and compensates the negative charges of the acidic surface groups more efficiently than Na⁺ or Li⁺, corresponding to the direct Hofmeister series according to stabilizing efficiency. Additional Hofmeister series alterations at low pH originate from reversal of the effective surface charge due to the proliferating adsorption of Cs⁺ [33]. At the same time, the Hofmeister series for anions remains essentially unchanged when varying the pH since the anion binding affinity remains unchanged as the surface carboxyl groups deprotonate (Table 1).

4. Conclusion

Predicting ion-surface interactions is challenging due to the entangled contributions of ions, surface functional groups and water. Consequently, to date no general theory exists that quantitatively predicts ion-surface interactions and encompasses hydrophobic, hydrophilic and charged surfaces. Insight into the microscopic origin of the Hofmeister series and its reversal can be gained from ion-surface interactions at atomistically resolved surfaces containing non-polar, polar and charged surface groups obtained from MD simulations. The calculated ion-surface free energy profiles include the contributions of ion hydration and direct ion-surface interactions explicitly and are the key to understand ion specific phenomena involving surfaces. Combining atomistically resolved ion-surface interactions with Poisson-Boltzmann theory allows us to provide a connection to macroscopic and experimentally measurable long-ranged forces which stabilize macromolecules in solution against precipitation. Based on the stabilization efficiency of anions and cations, reversal of the Hofmeister series is observed to be the rule rather than the exception. The ordering of the ions within the series can be altered by changing surface properties such as the sign of the surface charge, the surface hydrophobicity or when changing the chemical structure of acidic groups by increasing the pH. Given the resulting complex spectrum of direct, altered and reversed Hofmeister series, it is surprising that

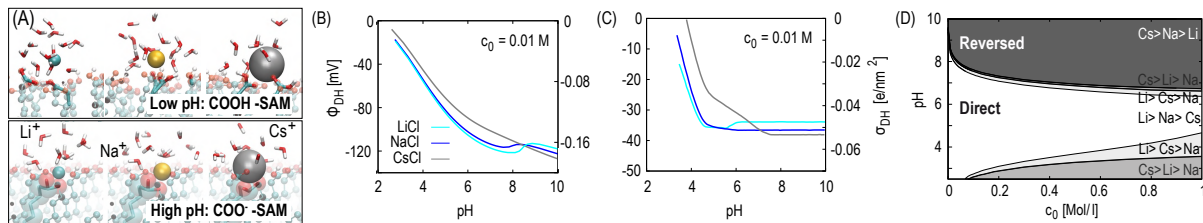


Figure 6: (A) Simulation snapshots of the cations Li^+ , Na^+ , and Cs^+ at the uncharged COOH-terminated surface at low pH (top) and at the charged COO^- -terminated surface at high pH (bottom). At the uncharged surface the cation-surface affinity follows the direct Hofmeister series: $\text{Cs}^+ > \text{Na}^+ > \text{Li}^+$. At the charged surface the cation-surface affinity is reversed and follows the reversed Hofmeister series: $\text{Li}^+ > \text{Na}^+ > \text{Cs}^+$. (B) Stabilizing repulsive force between surfaces containing carboxyl surface groups measured by the effective surface potential Φ_{DH} (left scale) and the equivalent effective surface charge σ_{DH} (right scale) as function of pH for a small bulk salt concentration $c_0 = 0.01$ M from PB modeling. (C) Φ_{DH} and σ_{DH} for silica surfaces dependent on pH obtained from AFM experiments. (D) Hofmeister phase diagram as function of pH and bulk salt concentration c_0 for surfaces covered by carboxyl groups. Colored areas denote regions featuring direct order (white), indirect order (black), and two different alterations. The ordering of the ions corresponds to their efficiency in stabilization according to σ_{DH} or Φ_{DH} . All calculations are done using the modified PB approach (i.e. restricted ionic density).

a robust ordering of the anions and cations is observed for many complex biomolecules including proteins. This is traced back to the fact that most proteins are negatively charged and ion binding is dominated by the presence of hydrophobic surface patches. What we have presented here is therefore only the beginning of a detailed understanding of ion specific phenomena for complex biologically relevant macromolecules. To complement our current comprehension of Hofmeister effects, a detailed insight into the ion-binding characteristics to a large variety of functional groups that are present on proteins, lipid bilayers or nucleic acids is needed [5, 9, 73]. In addition, a realistic modeling of complex molecular and multivalent ions is highly desirable but remains challenging even for divalent ions [74].

5. Acknowledgments

We acknowledge financial support from the Alexander von Humboldt foundation, the DFG via the SFB 1078 and the German-Israeli Foundation for Scientific Research and Development (GIF) in the project "Ion specific interactions between functionalized surfaces".

References

** outstanding interest, * special interest.

- [1] J. Traube, The attraction pressure, *J. Phys. Chem.* 14 (5) (1910) 452–470.
- [2] K. D. Collins, Ions from the Hofmeister series and osmolytes: effects on proteins in solution and in the crystallization process, *Methods* 34 (2004) 300–311.
- [3] W. Kunz, P. Lo Nostro, B. W. Ninham, The present state of affairs with Hofmeister effects, *Curr. Opin. Colloid Interface Sci.* 9 (1-2) (2004) 1 – 18.
- [4] C. L. Henry, C. N. Dalton, L. Scruton, V. S. J. Craig, Ion-specific coalescence of bubbles in mixed electrolyte solutions, *J. Phys. Chem. C* 111 (2) (2007) 1015–1023.
- [5] J. J. Garcia-Celma, L. Hatahet, W. Kunz, K. Fendler, Specific anion and cation binding to lipid membranes investigated on a solid supported membrane, *Langmuir* 23 (20) (2007) 10074–10080.
- [6] H. I. Petrache, T. Zemb, L. Belloni, V. A. Parsegian, Salt screening and specific ion adsorption determine neutral-lipid membrane interactions, *Proc. Natl. Acad. Sci. U.S.A.* 103 (21) (2006) 7982–7987.
- [7] Y. Zhang, P. S. Cremer, Interactions between macromolecules and ions: the Hofmeister series, *Curr. Opin. Chem. Biol.* 10 (6) (2006) 658–663.

* In this review, recent advances on identifying the mechanism of the Hofmeister series are summarized. The review provides clear evidence that Hofmeister phenomena result from direct interactions between ions and macromolecules and not from water structure effects.

- [8] W. Kunz, L. Belloni, O. Bernard, B. Ninham, Osmotic coefficients and surface tensions of aqueous electrolyte solutions: Role of dispersion forces, *J. Phys. Chem. B* 108 (7) (2004) 2398–2404.
- [9] N. Vlachy, M. Drechsler, J.-M. Verbavatz, D. Touraud, W. Kunz, Role of the surfactant headgroup on the counterion specificity in the micelle-to-vesicle transition through salt addition, *J. Colloid Interface Sci.* 319 (2) (2008) 542–548.
* The paper discusses the role of counter-ions on the micelle-to-vesicle transformation observed in experiments. It is shown that if the sulfate head group is replaced by a carboxylic group, the ordering the cations in the Hofmeister series is reversed.
- [10] F. Hofmeister, Zur Lehre von der Wirkung der Salze (About the science of the effect of salt), *Arch Exp Pathol Phar* 24 (24) (1888) 247–260.
- [11] A. Omta, M. Kropman, S. Woutersen, H. Bakker, Negligible effect of ions on the hydrogen-bond structure in liquid water, *Science* 301 (5631) (2003) 347–349.
- [12] J. Batchelor, A. Olteanu, A. Tripathy, G. Pielak, Impact of protein denaturants and stabilizers on water structure, *J. Am. Chem. Soc.* 126 (7) (2004) 1958–1961.
- [13] M. Gurau, S. Lim, E. Castellana, F. Albertorio, S. Kataoka, P. Cremer, On the mechanism of the Hofmeister effect, *J. Am. Chem. Soc.* 126 (34) (2004) 10522–10523.
- [14] W. Kunz, Specific ion effects in colloidal and biological systems, *Curr. Opin. Colloid Interface Sci.* 15 (1-2) (2010) 34 – 39.
- [15] L. M. Pegram, M. T. Record, Jr., Thermodynamic origin of Hofmeister ion effects, *J. Phys. Chem. B* 112 (31) (2008) 9428–9436.
* In this paper, a thermodynamic analysis is presented to predict Hofmeister salt effects on micelle formation and other processes from structural information. Based on the solubility of hydrocarbons and oligoamides, single ion partition coefficients are obtained which quantify accumulation or exclusion of cations and anions in the vicinity of molecular surfaces.
- [16] Y. Zhang, P. S. Cremer, Chemistry of Hofmeister Anions and Osmolytes, *Annu. Rev. Phys. Chem.* 61 (1) (2010) 63–83.
- [17] M. Boström, F. Tavares, S. Finet, F. Skouri-Panet, A. Tardieu, B. Ninham, Why forces between proteins follow different Hofmeister series for pH above and below pI, *Biophys. Chem.* 117 (3) (2005) 217–224.
* In this paper, a theoretical explanation of Hofmeister series reversal for proteins with pH below and above their pI is presented. In the theoretical model, the non-electrostatic interactions between the ion and the protein surface are included via an ionic dispersion interaction potential. Ion-specific and electrostatic forces are treated together consistently in nonlinear Poisson-Boltzmann theory.
- [18] H. Kim, E. Tuite, B. Norden, B. Ninham, Co-ion dependence of dna nuclease activity suggests hydrophobic cavitation as a potential source of activation energy, *Eur. Phys. J. E* 4 (4) (2001) 411–417.
- [19] Y. Zhang, P. S. Cremer, The inverse and direct Hofmeister series for lysozyme, *Proc. Natl. Acad. Sci. U.S.A.* 106 (36) (2009) 15249–15253.
** The paper shows that the inverse Hofmeister series is obtained for positively charged macromolecules like lysozyme only at relatively low salt concentrations. The series reverts into the direct Hofmeister series as the salt concentration is increased.
- [20] M. Dishon, O. Zohar, U. Sivan, From Repulsion to Attraction and Back to Repulsion: The Effect of NaCl, KCl, and CsCl on the Force between Silica Surfaces in Aqueous Solution, *Langmuir* 25 (5) (2009) 2831–2836.
* The paper shows results from precise AFM measurements for the force between silica surfaces in electrolyte solutions. With increasing salt concentration, the force changes from repulsion to attraction and eventually back to attraction, reflecting the transition from effectively negative to neutral and then to positive surface charges due to specific cation adsorption.
- [21] S. C. Flores, J. Kherb, P. S. Cremer, Direct and Reverse Hofmeister Effects on Interfacial Water Structure, *J. Phys. Chem. C* 116 (27) (2012) 14408–14413.
- [22] S. C. Flores, J. Kherb, N. Konelick, X. Chen, P. S. Cremer, The Effects of Hofmeister Cations at Negatively Charged Hydrophilic Surfaces, *J. Phys. Chem. C* 116 (9) (2012) 5730–5734.
- [23] J. Morag, M. Dishon, U. Sivan, The Governing Role of Surface Hydration in Ion Specific Adsorption to Silica: An AFM-Based Account of the Hofmeister Universality and its Reversal, *Langmuir* 29 (29) (2013) 6317–6322.
** The paper discusses the pH dependence of the ion specific force between silica surfaces. Precise AFM measurements provide insight into the Hofmeister order and its reversal and into the role of surface hydration and specific ion adsorption to silica.
- [24] M. Ries-Kautt, A. Ducruix, Relative effectiveness of various ions on the solubility and crystal growth of lysozyme, *J. Biol. Chem.* 264 (2) (1989) 745–748.
- [25] C. Carbonnaux, M. Ries-Kautt, A. Ducruix, Relative effectiveness of various anions on the solubility of acidic hypodermelineatum collagenase at pH 7.2, *Protein Sci.* 4 (10) (1995) 2123–2128.
- [26] S. Finet, F. Skouri-Panet, M. Casselyn, F. Bonnet, A. Tardieu, The Hofmeister effect as seen by SAXS in protein solutions, *Current Opinion in Colloid & Interface Science* 9 (1-2) (2004) 112 – 116.
* The paper discusses the effect of monovalent salts on biological macromolecules in solution by SAXS. It is shown that the Hofmeister series is direct/indirect for pH above/below the macromolecular pI.
- [27] T. López-León, M. J. Santander-Ortega, J. L. Ortega-Vinuesa, D. Bastos-González, Hofmeister Effects in Colloidal Systems: Influence of the Surface Nature, *J. Phys. Chem. C* 112 (41) (2008) 16060–16069.
** This paper shows experimental evidence that the Hofmeister series is not only reversed when changing the sign of the surface charge, but also when changing the nature of the surface from hydrophobic to hydrophilic. Detailed insight into the ranking of the ions is obtained by systematic measurements of the stability of colloidal particles with adjusted surface coatings.
- [28] T. López-León, A. B. Jódar-Reyes, D. Bastos-González, J. L. Ortega-Vinuesa, Hofmeister Effects in the Stability and

- Electrophoretic Mobility of Polystyrene Latex Particles, *J. Phys. Chem. B* 107 (24) (2003) 5696–5708.
- [29] T. López-León, A. Jódar-Reyes, J. Ortega-Vinuesa, D. Bastos-González, Hofmeister effects on the colloidal stability of an IgG-coated polystyrene latex, *J. Colloid Interface Sci.* 284 (1) (2005) 139–148.
- [30] J. Lyklema, Simple Hofmeister series, *Chem. Phys. Lett.* 467 (4-6) (2009) 217 – 222.
 ** This article reviews the Hofmeister series at well-defined water/solid interfaces. The series observed are not unique and the results provide an overview of direct and reversed series observed in different systems.
- [31] J. Lyklema, Lyotropic sequences in colloid stability revisited, *Advances in Colloid and Interface Science* 100-102 (2003) 1 – 12.
- [32] F. Dumont, J. Warlus, A. Watillon, Influence of the point of zero charge of titanium-dioxide hydrosols on the ionic adsorption sequences, *J. Colloid Interface Sci.* 138 (2) (1990) 543–554.
- [33] N. Schwierz, D. Horinek, R. R. Netz, Specific Ion Binding to Carboxylic Surface Groups and the pH Dependence of the Hofmeister Series, *Langmuir* 31 (1) (2015) 215–225.
 * This article discusses the pH dependent reversal of the Hofmeister series. Specific ion adsorption to carboxylic surface groups is quantified using molecular dynamics simulations and combined with Poisson-Boltzmann theory.
- [34] W. Kunz, *Specific Ion Effects*, 1st Edition, Wiley & Sons, Chichester, 2007.
- [35] W. Melander, C. Horvath, Salt effects on hydrophobic interactions in precipitation and chromatography of proteins: An interpretation of the lyotropic series, *Arch. Biochem. Biophys.* 183 (1) (1977) 200–215.
- [36] L. M. Pegram, M. T. Record, Jr., Quantifying accumulation or exclusion of H⁺, HO⁻, and Hofmeister salt ions near interfaces, *Chem. Phys. Lett.* 467 (1-3) (2008) 1–8.
- [37] R. Baldwin, How Hofmeister ion interactions affect protein stability, *Biophys. J.* 71 (4) (1996) 2056–2063.
- [38] P. Jungwirth, D. Tobias, Molecular structure of salt solutions: A new view of the interface with implications for heterogeneous atmospheric chemistry, *J. Phys. Chem. B* 105 (43) (2001) 10468–10472.
- [39] P. Jungwirth, D. Tobias, Ions at the air/water interface, *J. Phys. Chem. B* 106 (25) (2002) 6361–6373.
- [40] D. M. Huang, C. Cottin-Bizonne, C. Ybert, L. Bocquet, Aqueous electrolytes near hydrophobic surfaces: Dynamic effects of ion specificity and hydrodynamic slip, *Langmuir* 24 (4) (2008) 1442–1450.
- [41] D. Horinek, A. Herz, L. Vrbka, F. Sedlmeier, S. I. Mamatkulov, R. R. Netz, Specific ion adsorption at the air/water interface: The role of hydrophobic solvation, *Chem. Phys. Lett.* 479 (4-6) (2009) 173–183.
 * Specific ion adsorption at the air/water interface is investigated with molecular dynamics simulations in combination with Poisson-Boltzmann theory. The higher affinity of large anions for the interface is rationalized by hydrophobic solvation theory adapted to the air/water interface.
- [42] Y. Levin, A. P. Dos Santos, A. Diehl, Ions at the air-water interface: An end to a hundred-year-old mystery?, *Phys. Rev. Lett.* 103 (2009) 257802.
- [43] N. Schwierz, D. Horinek, R. R. Netz, Anionic and Cationic Hofmeister Effects on Hydrophobic and Hydrophilic Surfaces, *Langmuir* 29 (8) (2013) 2602 – 2614.
 ** This article discusses the full spectrum of direct, reversed and altered Hofmeister series for anions and cation dependent on surface charge and surface hydrophobicity. The ordering of the ions is quantified based on interfacial tension increments and long-ranged electrostatic forces.
- [44] D. Horinek, R. R. Netz, Specific ion adsorption at hydrophobic solid surfaces, *Phys. Rev. Lett.* 99 (22) (2007) 226104.
- [45] N. Schwierz, R. R. Netz, Effective Interaction between two Ion-Adsorbing Plates: Hofmeister Series and Salting-In/Salting-Out Phase Diagrams from a Global Mean-Field Analysis, *Langmuir* 28 (8) (2012) 3881–3886.
- [46] N. Schwierz, D. Horinek, R. R. Netz, Reversed Anionic Hofmeister Series: The Interplay of Surface Charge and Surface Polarity, *Langmuir* 26 (10) (2010) 7370–7379.
 ** This paper provides insight into the reversal of the anionic Hofmeister series when changing the sign of the surface charge or the surface hydrophobicity. By combining simulations in explicit water and Poisson-Boltzmann theory detailed microscopic insight into the origin of the series and its reversal is provided.
- [47] P. Jungwirth, D. J. Tobias, Specific ion effects at the air/water interface, *J. Chem. Rev.* 106 (4) (2006) 1259–1281.
 * This article reviews the results from computer simulations of ions at the air/water interface. A detailed comparison to continuum models and experimental observations, in particular spectroscopic experiments, is provided.
- [48] G. Luo, S. Malkova, J. Yoon, D. G. Schultz, B. Lin, M. Meron, I. Benjamin, P. Vanysek, M. L. Schlossman, Ion distributions near a liquid-liquid interface, *Science* 311 (5758) (2006) 216–218.
 * This article describes the methodology of using molecular dynamics simulations to calculate the potential of mean force for a single ion and to use it in a generalized Poisson-Boltzmann equation. This approach takes into account the liquid structure at the interface and around the ions and allows the authors to predict ionic distributions that agree with experimental measurements without any adjustable parameters.
- [49] W. R. P. Scott, P. H. Hunenberger, I. G. Tironi, A. E. Mark, S. R. Billeter, J. Fennel, A. E. Torda, T. Huber, P. Kruger, W. F. van Gunsteren, The gromos biomolecular simulation program package, *J. Phys. Chem. A* 103 (19) (1999) 3596–3607.
- [50] D. Horinek, S. I. Mamatkulov, R. R. Netz, Rational design of ion force fields based on thermodynamic solvation properties, *J. Chem. Phys.* 130 (12) (2009) 124507.
 * In this paper, a non-polarizable ionic force field is designed based on experimental solvation properties. The ionic force field parameters are chosen to yield accurate ion-water properties in classical MD simulation.
- [51] M. Fyta, I. Kalcher, J. Dzubiella, L. Vrbka, R. R. Netz, Ionic force field optimization based on single-ion and ion-pair solvation properties, *J. Chem. Phys.* 132 (2).
- [52] D. Van Der Spoel, E. Lindahl, B. Hess, G. Groenhof, A. E. Mark, H. J. C. Berendsen, Gromacs: Fast, flexible, and free, *J. Comput. Chem.* 26 (16) (2005) 1701 – 1718.
- [53] U. Essmann, L. Perera, M. L. Berkowitz, T. Darden, H. Lee, L. Pedersen, A smooth particle mesh ewald method, *J.*

- Chem. Phys. 103 (19) (1995) 8577–8593.
- [54] G. M. Torrie, J. P. Valleau, Nonphysical sampling distributions in monte carlo free-energy estimation: Umbrella sampling, *J. Comput. Phys.* 23 (2) (1977) 187 – 199.
 - [55] S. Kumar, J. M. Rosenberg, D. Bouzida, R. H. Swendsen, P. A. Kollman, Multidimensional free-energy calculations using the weighted histogram analysis method., *J. Comput. Chem.* 16 (11) (1995) 1339–1350.
 - [56] A. Haertl, J. A. Garrido, S. Nowy, R. Zimmermann, C. Werner, D. Horinek, R. Netz, M. Stutzmann, The ion sensitivity of surface conductive single crystalline diamond, *J. Am. Chem. Soc.* 129 (5) (2007) 1287–1292.
 - [57] J. Heyda, J. Pokorna, L. Vrbka, R. Vacha, B. Jagoda-Cwiklik, J. Konvalinka, P. Jungwirth, J. Vondrasek, Ion specific effects of sodium and potassium on the catalytic activity of hiv-1 protease, *Phys. Chem. Chem. Phys.* 11 (35) (2009) 7599–7604.
 - [58] J. Bikerman, Structure and capacity of electrical double layer., *Philos. Mag.* 33 (220, 7TH SERIES) (1942) 384–397.
 - [59] I. Borukhov, D. Andelman, H. Orland, Adsorption of large ions from an electrolyte solution: A modified poisson-boltzmann equation, *Electrochim. Acta* 46 (2-3) (2000) 221–229.
 - [60] D. Evans, H. Wennerström, *The Colloidal Domain: Where Physics, Chemistry, Biology and Technology Meet*, 2nd Edition, Wiley-VCH, 1999.
 - [61] A. Salis, M. Pinna, D. Bilanicova, M. Monduzzi, P. Lo Nostro, B. Ninham, Specific anion effects on glass electrode pH measurements of buffer solutions: Bulk and surface phenomena, *J. Phys. Chem. B* 110 (6) (2006) 2949–2956.
 - [62] P. H. von Hippel, K.-Y. Wong, Neutral salts: The generality of their effects on the stability of macromolecular conformations, *Science* 145 (3632) (1964) 577–580.
 - [63] M. Lund, P. Jungwirth, C. E. Woodward, Ion specific protein assembly and hydrophobic surface forces, *Phys. Rev. Lett.* 100 (25) (2008) 258105.
 - [64] P. Jungwirth, Spiers memorial lecture: Ions at aqueous interfaces, *Faraday Discuss.* 141 (2009) 9–30.
 - [65] K. Collins, Charge density-dependent strength of hydration and biological structure, *Biophys. J.* 72 (1) (1997) 65–76.
 - [66] D. J. Bonhuis, S. Gekle, R. R. Netz, Profile of the static permittivity tensor of water at interfaces: Consequences for capacitance, hydration interaction and ion adsorption, *Langmuir* 28 (20) (2012) 7679–7694.
 - [67] K. F. Rinne, S. Gekle, R. R. Netz, Ion-specific solvation water dynamics: Single water versus collective water effects, *The Journal of Physical Chemistry A* 118 (50) (2014) 11667–11677.
 - [68] E. R. A. Lima, M. Bostrom, N. Schwierz, B. E. Sernelius, F. W. Tavares, Attractive double-layer forces between neutral hydrophobic and neutral hydrophilic surfaces, *Phys. Rev. E* 84 (6, 1).
 - [69] T. Robertson, Contributions to the theory of the mode of action of inorganic salts upon proteins in solution, *J. Biol. Chem.* 9 (3) (1911) 303–326.
 - [70] A. Green, Studies in the physical chemistry of the proteins x. the solubility of hemoglobin in solutions of chlorides and sulfates of varying concentration, *J. Biol. Chem.* 95 (1) (1932) 47–66.
 - [71] W. Poillon, J. Bertles, Deoxygenated sickle hemoglobin - effects of lyotropic salt on its solubility, *J. Biol. Chem.* 254 (9) (1979) 3462–3467.
 - [72] P. Nandi, D. Robinson, Effects of salts on free-energies of nonpolar groups in model peptides, *J. Am. Chem. Soc.* 94 (4) (1972) 1308–1315.
 - [73] N. Vlachy, B. Jagoda-Cwiklik, R. Vácha, D. Touraud, P. Jungwirth, W. Kunz, Hofmeister series and specific interactions of charged headgroups with aqueous ions, *Advances in Colloid and Interface Science* 146 (1-2) (2009) 42 – 47.
- ** In this review, specific interactions of ions with charged surfactants and lipid head groups are discussed based on experimental and computational results. This comprehensive data set in combination with the law of matching water affinities allows the authors to predict ion specific interactions qualitatively for a wide range of systems.
- [74] S. Mamatkulov, M. Fyta, R. R. Netz, Force fields for divalent cations based on single-ion and ion-pair properties, *J. Chem. Phys.* 138 (2).